where $r = \sqrt{x^2 + y^2}$, R is the radius of the sphere, and x and y are Cartesian coordinates with origin at the center of the sphere.

From these equations, the expression for total pressure can be derived. It is

$$\frac{p_t - p_{t\infty}}{\frac{1}{2}\rho U_\infty^2} = \left[\frac{3}{4}\frac{Rx^2}{r^3}\left(\frac{R^2}{r^2} - 1\right) - \frac{1}{4}\frac{R}{r}\left(3 + \frac{R^2}{r^2}\right) + 1\right]^2 + \left[\frac{3}{4}\frac{Rxy}{r^3}\left(\frac{R^2}{r^2} - 1\right)\right]^2 - 1 - \frac{6}{Re}\frac{R^2 x}{r^3} \tag{19}$$

where $Re \equiv (2\rho U_\infty R)/\mu$ and $p_{t\infty}$ is the value of total pressure far upstream.

Contours of $(p_t - p_{t\infty})/\frac{1}{2}\rho U_\infty^2$ given by Eq. (19) are plotted in Fig. 5 for $Re = 1$, above which the exact solution becomes invalid. Once again it is clear that the total pressure can undergo a local increase that in this case is substantial. Here also the rise in total pressure is proportional to the viscosity as can be deduced from Eq. (19).

Conclusions

The common assumption that the total pressure can only decrease everywhere in frictional flow is an erroneous one. It is shown by examining the total pressure transport equation that stresses can, in principle, result in a local rise in total pressure; the mechanism by which this happens is the redistribution of mechanical energy by the action of these stresses. This is demonstrated for two classical flow cases for which exact solutions exist. It is found that the rise in total pressure is directly proportional to the viscosity. This implies that total pressure could indeed increase in turbulent flows more than in laminar ones becuse of the higher effective viscosity/stresses.

References

[1]Cebeci, T., and Bradshaw, P., *Momentum Transfer in Boundary Layers,* Hemisphere, New York, 1977.

[2]Schlichting, H. *Boundary Layer Theory,* McGraw-Hill, New York, 1966.

Relationship Between Transition and Modes of Instability in High-Speed Boundary Layers

Jamal A. Masad
High Technology Corporation,
Hampton, Virginia 23666

Introduction

A RELATIONSHIP exists between the different laminar-flow instability mechanisms in both low- and high-speed boundary-layer flows on aerodynamic surfaces and the breakdown of the laminar flow to turbulence. However, the details of this relationship are not well understood, particularly for high-speed flows. The most common approach for relating instability to transition is the use of the empirical N factor method, in which transition is assumed to occur whenever the integral of the linear growth rate of any instability wave reaches a certain value that is close to 9 in two-dimensional flows. In high-speed flows, the instability is complicated by the possible existence of higher modes of instability in addition to the single mode of instability [the Tollmien–Schlichting (T-S) wave] that exists in low-speed flows.

Received Oct. 29, 1993; revision received May 10, 1994; accepted for publication May 10, 1994.

*Research Scientist. Senior Member AIAA.

Mack[1] determined through numerical studies that whenever the mean flow relative to the disturbance phase velocity is supersonic over some portion of the boundary-layer profile, an infinite number of wave numbers corresponds to a single phase velocity. He called the additional disturbances "the higher modes." Mack called the first of the higher modes the second mode, which is also referred to in the literature as the Mack mode. The originally known mode that corresponds to that in incompressible flow is called the first mode. In this work, we examine the relationship between transition and modes of linear instability in both adiabatic and cooled high-speed flows over a flat plate.

Notation

In all calculations and results presented in this work, the quasi-parallel spatial stability theory is used, and therefore the frequency of the disturbance is real, whereas the spatial eigenvalue is complex. The growth rate of the wave is denoted by $-\alpha_i$, and it is made nondimensional with respect to the length scale $\delta_r^* = \sqrt{\nu_\infty^* x^*/U_\infty^*}$ such that $\alpha = \alpha^* \delta_r^*$. The dimensional freestream kinematic viscosity is denoted by ν_∞^*. The spanwise wave number parameter B is defined as $B = 1000\beta/R$ and is fixed for the same physical wave as it propagates downstream. The nondimensional spanwise wave number is $\beta = \beta^* \delta_r^*$, and β^* is the dimensional spanwise wave number of the wave. The stability Reynolds number is $R = U_\infty^* \delta_r^*/\nu_\infty^* = \sqrt{Re_x}$. The frequency parameter F is defined as $F = 2\pi f^* \nu_\infty^*/U_\infty^{*2}$, where f^* is the dimensional frequency in cycles per second (Hz) and is related to the dimensional circular frequency ω^* through $\omega^* = 2\pi f^*$. Therefore, $\omega = \omega^* \delta_r^*/U_\infty^*$ is related to F through $\omega = FR$. The specific heat at constant pressure is assumed constant, and the Prandtl number is fixed at 0.72. The dynamic viscosity varies with temperature in accordance to the Sutherland formula.

From both a practical and an experimental point of view, the wall temperature is more easily fixed than the heat flux. Therefore, we express the level of heat transfer by specifying the ratio T_w/T_{ad}, where T_w is the actual wall temperature made nondimensional with respect to T_∞^*, and T_{ad} is the adiabatic wall temperature also made nondimensional with respect to T_∞^*. If $T_w/T_{ad} = 1$, then the wall is adiabatic; if $T_w/T_{ad} < 1$, then the wall is cooled; if $T_w/T_{ad} > 1$, then the wall is heated. For first-mode waves in supersonic adiabatic boundary layers, Mack[1] found that oblique three-dimensional waves are more unstable than two-dimensional waves. Cooling has a stabilizing influence on the two- and three-dimensional first-mode waves.

Results

The most amplified second-mode waves are two-dimensional. Although cooling stabilizes first-mode waves, it has the opposite effect on the most amplified (over all frequencies) second-mode waves and destabilizes them. Heating, rather than cooling, stabilizes second-mode waves. Because second-mode waves are significant at high Mach numbers where the adiabatic wall temperatures are already large in terms of existing materials, heating is not practical in stabilizing the flow at high Mach numbers. Shaw and Duck[2] showed that at a freestream Mach number of 4 and when the cooling level exceeds a certain value, the inviscid maximum growth rate of second-mode waves starts decreasing. Our viscous calculations at the same Mach number, $R = 1.5 \times 10^3$, and $T_\infty = 120$ K show a similar effect (Fig. 1). However, our viscous calculations at $R = 1.5 \times 10^3$ and at the hypersonic Mach number of 10 showed that this reversal in the effect of cooling does not take place even with cooling levels as low as $T_w/T_{ad} = 0.02$ at $T_\infty = 50$ K and $T_w/T_{ad} = 0.01$ at $T_\infty = 300$ K.

When the first mode is responsible for transition, cooling the surface delays transition. However, cooling the surface destabilizes the second mode. Beyond a certain level of cooling, the second mode causes transition, and further cooling causes the location of transition to move upstream (Fig. 2). The results shown in Fig. 2 indicate clearly that by applying cooling to the flat plate, the instability mode responsible for transition switches from a first to a second mode. As the flat plate is cooled, the predicted transition location moves downstream and, with sufficient cooling, starts to move upstream. In Fig. 2 at a Mach number of 5, the switch from the first to the

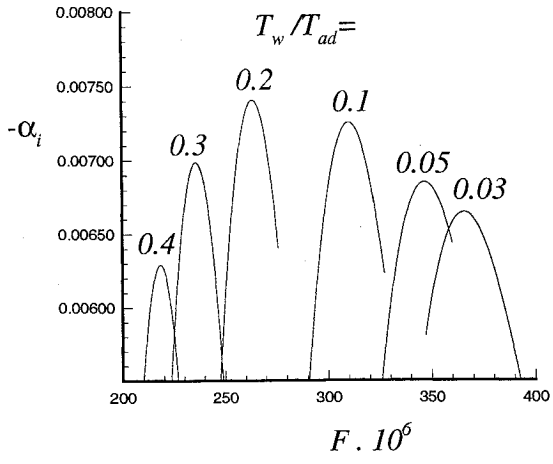

Fig. 1 Variation of growth rates of two-dimensional second-mode waves with frequency at $M_\infty = 4$, $R = 1.5 \times 10^3$, and $T_\infty = 120$ K.

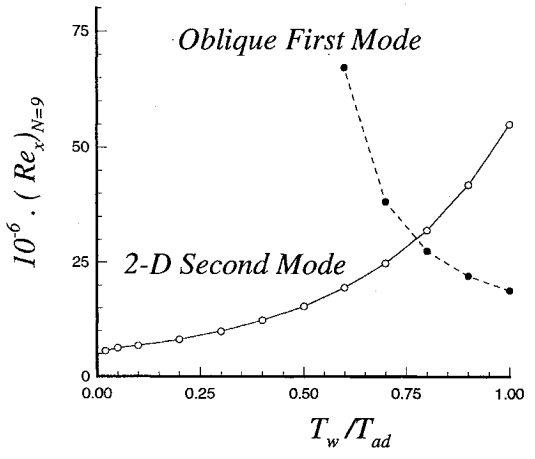

Fig. 2 Variation of predicted transition location with wall temperature at $M_\infty = 5.0$, $T_\infty = 300$ K, and $Pr = 0.72$.

second mode of instability as the cause of transition occurs at a level of surface temperature between $T_w/T_{ad} = 0.7$ and 0.8. This level is expected to decrease as the freestream Mach number decreases. In fact, recent calculations by Mack[3] at a freestream Mach number of 3 and a freestream temperature of 217 K show the reversal that occurred in Fig. 2 to take place at $T_w/T_{ad} \approx 0.6$. Figure 2 clearly shows that, when both modes of instability are considered, the effect of cooling on changing the predicted transition location becomes less significant. We note here that although the maximum growth rate of second-mode waves decreases when the cooling level exceeds a certain high value (Fig. 1), a high level of cooling does not cause the transition location to move downstream when transition is assumed to occur due to a single frequency. The maximum growth rates in Fig. 1 are associated with very high frequencies that do not contribute to transition except within an envelope method in which the local maximum growth rate (over all frequencies) is integrated with respect to R to compute the N factor. Only in that context we get a downstream movement of transition location at high levels of cooling.

Lysenko[4] presented results similar to those presented in Fig. 2 but at a Mach number of 4 and for flow past a cone. Lysenko's results were obtained by solving the stability equations in the Dunn–Lin[5] approximation.

In Fig. 2, the points where the actual calculations were made are denoted by circles; the circles are joined by straight lines. The calculations were performed by first fixing the frequency F and the spanwise wave number parameter B and computing the location (the Reynolds number) where the N factor reached a value of 9. With B fixed, F was then varied, and the new location where the N factor reached 9 was computed, and so on. The value of F that resulted in the lowest Reynolds number at which the N factor reached 9

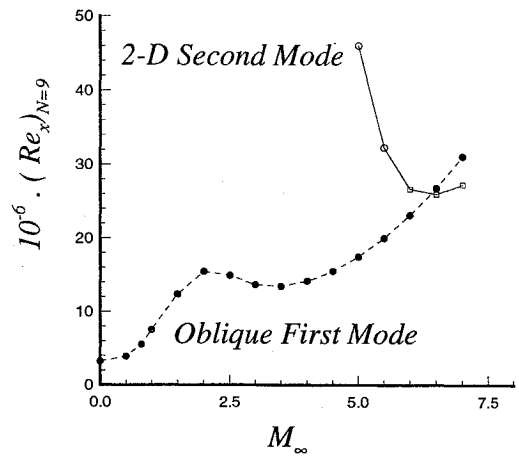

Fig. 3 Variation of predicted transition location in adiabatic flow with freestream Mach number at $T_\infty = 150$ K and $Pr = 0.72$.

was then fixed, and B was varied to compute the lowest Reynolds number at which N reached 9. With computed value of B fixed, F was varied, and so on, until both F and B remained fixed within preset tolerances. The tolerance (step)in F was 10^{-6}, and the step in B was 0.001. Because the most amplified second-mode waves are two-dimensional, a maximization over B is not necessary when these waves are considered. A similar approach is used for the results in Fig. 3.

A significant result seen in Fig. 2 is that for adiabatic flow with a freestream Mach number of 5 the predicted transition is caused by the first mode of instability, although the maximum growth rate of second-mode waves at this Mach number exceeds that of first-mode waves by a large amount. The reason for this difference is that the streamwise extent of the unstable range of first-mode instability waves is much longer than that of second-mode waves. Therefore, the integrated growth rate (N factor) of first-mode waves reaches the value 9 before that of second-mode waves.

The value of the freestream Mach number in adiabatic flow at which the cause of transition becomes the second mode of instability is of interest. To find this value, the predicted transition location was computed with the N factor criterion over a range of Mach numbers that extends from 0 to 7. The results are shown in Fig. 3. The squares in Fig. 3 indicate conditions where transition is caused by a combination of the two-dimensional first and second modes of instability. At the considered freestream temperature of 150 K and a Prandtl number of 0.72, the predicted transition is caused by a combination of two-dimensional first and second modes of instability at a freestream Mach number between 6 and 6.5. In Fig. 3, the N-factor criterion predicts that compressibility destabilizes at freestream Mach numbers in the range of 2–3.5. In this range, an increasing Mach number shifts the predicted transition location upstream. This result is significant for laminar-flow control (LFC) applications. For supersonic transport, the optimal Mach number appears to be approximately 2 for LFC consideration.

When the transition location predicted with the N-factor criterion moves upstream, the corresponding most dangerous frequency increases. This result occurs when transition is caused by either first or second mode of instability. An exception to this is when transition is caused by a combination of two-dimensional first and second modes of instability (the squares in Fig. 3). Except for subsonic flows where the most amplified first-mode waves are two-dimensional, the upstream movement of the transition location is associated with an increase in the value of the spanwise wave number parameter when the first mode is responsible for transition. The calculations of Lysenko[4] for flow past a cone and using the stability equations with the Dunn–Lin[5] approximation show results similar to those in Fig. 3. Results similar to those in Fig. 3 and for first-mode waves have been reported by Mack[6] and Arnal et al.[7]

Acknowledgments

This research is supported by the Theoretical Flow Physics Branch, Fluid Mechanics Division, NASA Langley Research Cen-

ter, Hampton, VA, under Contract NAS1-19299. The discussions with Mujeeb Malik are greatly appreciated.

References

[1]Mack, L. M., "Boundary-Layer Stability Theory," Jet Propulsion Lab., Document 900-277, Rev. A, Pasadena, CA, 1969.

[2]Shaw, S. J., and Duck, P. W., "The Inviscid Stability of Supersonic Flow Past Heated or Cooled Axisymmetric Bodies," *Physics of Fluids A*, Vol. 4, No. 7, 1992, pp. 1541–1557.

[3]Mack, L. M., "Effect of Cooling on Boundary-Layer Stability at Mach Number 3," *Instabilities and Turbulence in Engineering Flows*, edited by D. E. Ashpis, T. B. Gatski, and R. Hirsh, Kluwer Academic, Norwell, MA, 1993, pp. 175–188.

[4]Lysenko, V. I., "The Role of the First and Second Modes in Compressible Boundary-Layer Transition," *Applied Dynamics*, 1986, pp. 809–812.

[5]Lin, C. C., *The Theory of Hydrodynamic Stability*, Cambridge Univ. Press, Cambridge, England, UK, 1955.

[6]Mack, L. M., "Linear Stability Theory and the Problem of Supersonic Boundary-Layer Transition," *AIAA Journal*, Vol. 13, No. 3, 1975, pp. 278–289.

[7]Arnal, D., Vignau, F., and Laburthe, F., "Recent Supersonic Transition Studies with Emphasis on the Swept Cylinder Case," *Boundary Layer Transition & Control, Proceedings of the Boundary Layer Transition and Control Conference* (Cambridge, 1991), Royal Aeronautical Society, ISBN 0903409860, 1991.

Dynamic Thermoelastic Coupling Effects in a Rod

Dan Givoli* and Omri Rand†
Technion—Israel Institute of Technology, Haifa 32000, Israel

Nomenclature

A = cross-sectional area of the rod
C = specific heat
c = coefficient of externally induced viscous damping (friction with air)
E = Young's modulus
F = given distributed load (force per unit length)
L = length of rod
Q = given incident heat flux (power per unit volume)
T_0 = reference temperature in which the rod is undeformed
T = temperature above reference temperature T_0
U = axial displacement
α = coefficient of thermal expansion
δ = thermoelastic coupling coefficient
κ = thermal conductivity
ρ = mass density
ω = temporal frequency

Introduction

THE prediction of the dynamic response of thermally loaded elastic structures is of considerable importance in aerospace engineering and has been the subject of intensive research. In most cases the uncoupled equations of thermoelasticity have been considered, where the temperature field induces strains in the elastic body, but the elastic deformation is assumed not to affect the temperature field in turn. However, in some works the thermoelastic coupling effects have been included. The underlying principles and governing equations of linear coupled thermoelasticity are reviewed, e.g., by Nowacki.[1]

The thermoelastic coupling term in the heat equation acts like a thermal source that is proportional to the strain rate. Thus, a nonzero strain rate at a point in the material produces some change in the heat flux. This coupling effect is a linear dynamic effect. There are also additional types of thermoelastic coupling effects that are inherently nonlinear. One such effect occurs when the incident heat flux depends on the orientation of the structural members, as typical to space structure applications; see Givoli and Rand[2] and Rand and Givoli.[3] However, in this Note we shall be concerned with linear thermoelastic coupling.

Analytic solutions to coupled thermoelastic problems were considered by various authors; e.g., see Boley and Tolins,[4] Bahar and Hetnarski,[5] Takeuti et al.,[6] and Atkinson.[7] Numerical methods for coupled thermoelastic problems were also proposed. Some of the recent works are by Kasti et al.[8] and Farhat et al.[9]

Although it is widely known that thermoelastic coupling effects may be neglected in many applications, they may become important in some special cases. The purpose of this Note is to characterize the conditions under which thermoelastic coupling effects in a rod become relatively significant and to discuss the importance of these effects in aerospace applications.

Time-Harmonic Coupled Thermoelasticity

We consider the coupled axial heat flow and elastic deformation in a rod of length L. The thermal and elastic material behavior is assumed to be linear and the deformation to be small. We denote the axial coordinate by x and time by t.

To write the governing equations in a nondimensional form, we define the nondimensional variables and parameters,

$$\xi = x/L, \qquad \tau = \kappa t/(\rho C L^2)$$
$$\bar{T}(\xi,\tau) = T/T_0, \qquad \bar{U}(\xi,\tau) = U/L \tag{1}$$

$$\bar{\delta} = \frac{\delta}{T_0 \rho C}, \qquad \bar{Q} = \frac{L^2 Q}{\kappa T_0}, \qquad \bar{\rho} = \frac{\kappa^2 \rho}{(\rho C)^2 E L^2}$$
$$\bar{c} = \frac{\kappa c}{\rho C E}, \qquad \bar{\alpha} = T_0 \alpha, \qquad \bar{F} = \frac{LF}{EA} \tag{2}$$

Then the thermoelastic equations in nondimensional form are

$$\bar{T}_\tau = \bar{T}_{\xi\xi} - \bar{\delta}\bar{U}_{\xi\tau} + \bar{Q}(\xi,\tau) \tag{3}$$

$$\bar{\rho}\bar{U}_{\tau\tau} + \bar{c}\bar{U}_\tau = \bar{U}_{\xi\xi} - \bar{\alpha}\bar{T}_\xi + \bar{F}(\xi,\tau) \tag{4}$$

These equations hold in the unit interval $0 < \xi < 1$. The subscripts τ and ξ indicate partial differentiation. In what follows we shall concentrate on the thermally driven case where $\bar{F} \equiv 0$ in Eq. (4), as typical for example in space structure applications.

We now apply the Fourier transform in τ to Eqs. (3) and (4). This yields the thermoelastic equations in terms of ξ alone for a fixed temporal frequency ω. (We remark that it is also possible to apply the Laplace transform in τ, but this turns out to lead to more complicated mathematical expressions.) We define the nondimensional frequency $\bar{\omega}$ by requiring that $\omega t = \bar{\omega}\tau$, which leads to $\bar{\omega} = \rho C L^2 \omega/\kappa$. Denoting by $q(\xi)$, $T(\xi)$, and $u(\xi)$ the complex-valued Fourier transforms corresponding to $\bar{Q}$, $\bar{T}$, and $\bar{U}$, respectively, we obtain the following two equations for T and u:

$$T'' - i\bar{\omega}T - i\bar{\omega}\bar{\delta}u' + q = 0 \tag{5}$$

$$u'' + (\bar{\omega}^2\bar{\rho} - i\bar{\omega}\bar{c})u - \bar{\alpha}T' = 0 \tag{6}$$

where a prime indicates differentiation with respect to ξ. Equations (5) and (6) are accompanied by appropriate boundary conditions to complete the statement of the problem. Generally, unless $q(\xi)$ in Eq. (5) is especially simple, a particular analytic solution may be

Received Feb. 10, 1994; revision received Aug. 21, 1994; accepted for publication Aug 23, 1994;

*M. S. Geltman Senior Lecturer, Department of Aerospace Engineering.
†Senior Lecturer, Department of Aerospace Engineering; currently on leave at NASA Ames Research Center, M/S 219-3, Moffett Field, CA 94035.